This is the accepted manuscript made available via CHORUS. The article has been published as:

Absorption of microwaves by random-anisotropy magnets

Dmitry A. Garanin and Eugene M. Chudnovsky

Phys. Rev. B **103**, 214414 — Published 4 June 2021

DOI: 10.1103/PhysRevB.103.214414

Absorption of Microwaves by Random-Anisotropy Magnets

Dmitry A. Garanin and Eugene M. Chudnovsky
Physics Department, Herbert H. Lehman College and Graduate School, The City University of New York, 250 Bedford Park Boulevard West, Bronx, New York 10468-1589, USA
(Dated: May 24, 2021)

Microscopic model of the interaction of spins with a microwave field in a random-anisotropy magnet has been developed. Numerical results show that microwave absorption occurs in a broad range of frequencies due to the distribution of ferromagnetically correlated regions on sizes and effective anisotropy. That distribution is also responsible for the weak dependence of the absorption on the damping. At a fixed frequency of the ac-field spin oscillations are localized inside isolated correlated regions. Scaling of the peak absorption frequency agrees with the theory based upon Imry-Ma argument. The effect of the dimensionality of the system related to microwave absorption by thin amorphous magnetic wires and foils has been studied.

I. INTRODUCTION

In conventional ferromagnets the ac field can induce the uniform ferromagnetic resonance (FMR) and/or excite spin waves with a finite wave vector. In the presence of strong disorder in the local orientation of spins, however, that exists in spin glasses and amorphous ferromagnets, spin waves must be localized while the existence of the FMR becomes non-obvious. On general grounds one should expect that random magnets would exhibit absorption of the ac power in a broad frequency range that would narrow down when spins become aligned on increasing the external magnetic field.

Collective excitation modes have been observed in random magnets in the past[1–3]. In spin-glasses they were attributed[4] to the random anisotropy arising from Dzyaloshinskii-Moriya interaction and analyzed[5] within hydrodynamic theory[6,7]. Later Suran et al. studied collective modes in amorphous ferromagnets with random local magnetic anisotropy[8] and reported evidence of their localization[9]. Longitudinal, transverse and mixed modes have been observed in thin amorphous films. Detailed analysis of these experiments, accompanied by analytical theory of the uniform spin resonance in the random anisotropy (RA) ferromagnet in a nearly saturating magnetic field, has been recently given by Saslow and Sun[10]. Experimental evidence of localized spin excitations and micromagnetic models of the observed phenomena have also been reported in inhomogeneous thin magnetic films[11], submicron magnetic heterostructures[12], and in films where inhomogeneous magnetic field was generated by a tip of a force microscope[13].

A rigorous approach to this problem in RA ferromagnets requires investigation of the oscillation dynamics of a system of a large number of strongly interacting spins in a random potential landscape. While it was not possible at the time when most of the above-mentioned work on RA magnets was performed, the capabilities of modern computers allow one to address this problem numerically in great detail. Such a study must be worth pursuing because of the absence of the rigorous analytical theory of random magnets and also with an eye on their applications as microwave absorbers.

In this paper we consider the dynamics of an amorphous ferromagnet consisting of up to half-million spins within the RA model. It assumes (see, e.g., Refs. 14–16 and references therein) that spins interact via ferromagnetic exchange but that directions of local magnetic anisotropy axes are randomly distributed from one spin to another. In the past this model was successfully applied to the description of static properties of amorphous magnets, such as the ferromagnetic correlation length, zero-field susceptibility, the approach to saturation, etc.[17].

The essence of the RA model can be explained in the following terms. The ferromagnetic exchange tends to align the spins in one direction but it has no preferred direction. In the absence of the magnetic field, such direction in a crystalline body is determined by the magnetic anisotropy that arises from the violation of the rotational symmetry by the crystal lattice. Still, due to the time reversal symmetry, any two states with opposite directions of the magnetization have the same energy. In a macroscopic magnet this leads to the formation of ferromagnetically aligned magnetic domains. Magnetic particles of size below one micron typically consist of one such domain.

This changes in an amorphous magnet. If no material anisotropy was introduced by a manufacturing process, such a magnet would be lacking global anisotropy axes. Random on-site magnetic anisotropy disturbs the local ferromagnetic order but cannot break it at the atomic scale a because the RA energy per site, D_R, is small compared to the exchange energy J. The resulting magnetic state can be understood within the framework developed in the seminal papers of Larkin[18], and Imry and Ma[19]. Due to random local pushes from the RA the magnetization wonders around the magnet at the nanoscale in a random-walk manner (see Fig. 1), with the ferromagnetic correlation length given by $R_f/a \propto (J/D_R)^{2/(4-d)}$, where d is the dimensionality of the system.

This statement, known as the Imry-Ma (IM) argument, works for many systems with quenched randomness, such as disordered antiferromagnets[20], flux lattices in superconductors[21], charge-density waves[22], liquid crystals and polymers[23,24], and superfluid ^{3}He-A in

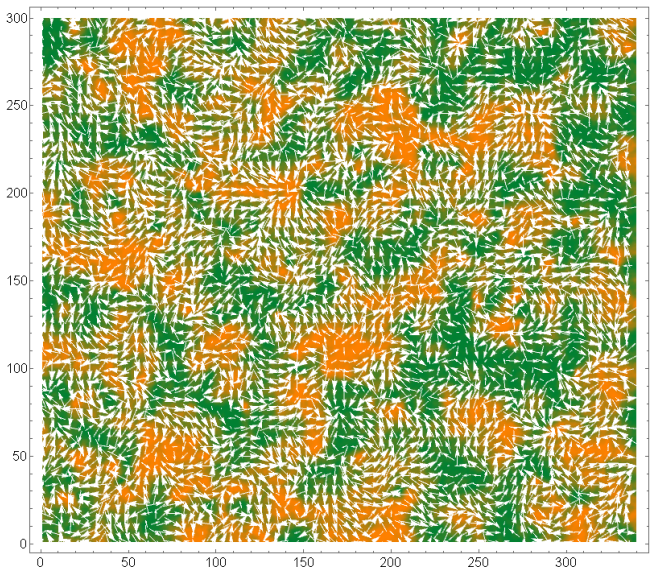

Figure 1: Spin configuration in a 2D RA ferromagnet obtained by relaxation from random initial orientations of three-component Heisenberg spins. Spins form correlated regions - Imry-Ma domains. The color coding reflects the sign of the out-of-plane s_z component of the spin, with orange/green corresponding to positive/negative. The in-plane spin components s_x, s_y are shown by white arrows.

aerogel[25]. In the case of the RA ferromagnet it suggests that the RA, no matter how weak, breaks the long range ferromagnetic order for $d = 1, 2, 3$, although the order can persist locally on the scale R_f that can be large compared to the interatomic distance a if $D_R \ll J$. For the same ratio D_R/J, the lower is the dimensionality of the system the smaller is the correlated region. (Formally, the long-range order is restored in higher dimensions, $d = 4, 5, ...$)

A fundamental feature of the RA model is that it can be rescaled in terms of spin blocks of size $r > a$ with the effective strength of random anisotropy $D'_R \sim D_R(a/r)^{d/2}$ and the effective exchange $J' \sim J(a/r)^2$ up to the size r at which $D'_R \sim J'$, which is the essence of the IM argument. This can be useful for numerical work but it also means that the model is intrinsically non-perturbative. It describes a strongly correlated system that cannot be treated perturbatively on small D_R/J. The latter is evidenced by the IM result for the ferromagnetic correlation length R_f.

One deficiency of the IM model is that it ignores topological defects[26] (apparent in Fig. 1) that lead to metastability. It was recently argued that random field (RF) converts a conventional ferromagnet into a topological glass in which ferromagnetically correlated regions (often called IM domains) possess non zero topological charges[27]. Although this argument was made for the RF rather than the RA, the two models have much in common due to the fact that the RA creates a local anisotropy field that acts on spins similarly to the RF. The RA model, however, is more nonlinear than the RF model. High metastability, history dependence, and memory effects[28] exhibited by ferromagnets with random magnetic anisotropy reveal complex non-ergodic temporal behavior typical of spin glasses[29].

Fueled by potential applications, there has been a large body of recent experimental research on the absorption of microwave radiation by nanocomposites comprised of magnetic nanoparticles of various shapes and dimensions, embedded in dielectric matrices[30]. With the use of more and more exotic shapes and materials, the complexity of such systems has increased dramatically in recent years[31–33] but their evaluation as microwave absorbers has been largely empirical and often a matter of luck rather than driven by theory.

Here we investigate the microwave absorption by the RA magnet in a zero external field. This case is the least obvious from the theoretical point of view and the least studied in experiments, although it must be the most interesting one for applications. We consider the model in which the ferromagnetic correlation length is dominated by the RA that is large compared to the local dipolar fields. As has been discussed above, static properties of this model were intensively investigated in the past and good agreement with experiment was achieved. However, theoretical studies of the dynamics were scarce. Our goal is to fill that gap and try to understand the fundamental physics of the absorption of the ac power by the random magnet without focusing on material science. The reference to microwaves throughout the paper is determined by the outcome: The peak absorption happens to be in the microwave range due to the typical strength of the magnetic anisotropy.

We should emphasize that this problem is noticeably different from the microwave absorption by a nanocomposite. Coated magnetic particles or particles dissolved in a dielectric medium are absorbing the ac power more or less independently when neglecting weak dipole-dipole interaction between them. On the contrary, in the amorphous ferromagnet all spins are coupled by the strong exchange interaction and they respond to the ac field collectively. Metastability and magnetic hysteresis exhibited by the RA magnet[16] makes such response highly nontrivial.

Here, we study the regime of the linear energy transfer from the input mode (the ac field) into a continuum of magnetic modes. Linear resonance transitions require a small amplitude of the ac field that is the case in many practical situations. In the linear regime, transitions between different metastable states of the random magnet are rare, most of the spins are precessing near their local energy minima. The physics of the linear energy transfer into the continuum is similar for both classical and quantum systems (Fermi's "Golden rule").

Our most interesting observation is that the absorption of the microwave power in the RA magnet is dominated by spin oscillations localized inside well-separated ferromagnetically correlated regions (IM domains) that at a given frequency are in resonance with the microwave

field. In that sense there is a similarity with a nanocomposite where certain particles react resonantly to the ac field of a given frequency. However, the number of such areas in a random magnet must be greater due to the higher concentration of spins.

The paper is organized as follows. The RA model and the numerical method for computing the absorption of the ac power are introduced in Section II. Results of the computations are given in Section III. Interpretation of the results, supported by snapshots of oscillating spins, is suggested in Section IV. Estimates of the absorbed power and implications of our findings for experiments are discussed in Section V.

II. THE MODEL AND NUMERICAL METHOD

We consider classical Heisenberg RA model described by the Hamiltonian

$$\mathcal{H} = -\frac{J}{2}\sum_{i,j}\mathbf{s}_i\cdot\mathbf{s}_j - \frac{D_R}{2}\sum_i(\mathbf{n}_i\cdot\mathbf{s}_i)^2 - \mathbf{h}(t)\cdot\sum_i\mathbf{s}_i, \quad (1)$$

where the first sum is over nearest neighbors, $\mathbf{s}_i$ is a three component spin of a constant length s, D_R is the strength of the easy axis RA in energy units, $\mathbf{n}_i$ is a three-component unit vector having random direction at each lattice site, and $\mathbf{h}(t) = \mathbf{h}_0\sin(\omega t)$ is the ac magnetic field in energy units. We assume ferromagnetic exchange, $J > 0$. Factor $1/2$ in front of the first term is needed to count the exchange interaction Js^2 between each pair of spins once. In our numerical work we consider a chain of equally spaced spins in 1D, a square lattice in 2D, and a cubic lattice in 3D. For the real atomic lattice of square or cubic symmetry the single-ion anisotropy of the form $-(\mathbf{n}\cdot\mathbf{s})^2$ would be absent, the first non-vanishing anisotropy terms would be fourth power on spin components. However, in our case the choice of the lattice is merely a computational tool that should not affect our conclusions.

The last term in Eq. (1) describes Zeeman interaction of the spins with the ac magnetic field of amplitude $\mathbf{h}_0$ and frequency ω. We assume that the wavelength of the electromagnetic radiation is large compared to the size of the system, so that the time-dependent field acting on the spins is uniform in space. This corresponds to situations of practical interest when the microwave radiation is incident to a thin dielectric layer containing random magnets.

As in microscopic studies of static properties of random magnets[14,17,26], we assume that in the absence of net magnetization the dynamics of the spins is dominated by the local exchange and the effective random magnetic anisotropy. The latter is determined by the amorphous structure factor or the size of the grain in a sintered material. It is typically large compared to the dipole-dipole interaction (DDI) between the spins. Adding DDI to the problem would have resulted in a considerable slowdown of the numerical procedure since the study of RA ferromagnets requires system of size large compared to the ferromagnetic correlation length. It would be justified only if DDI was significantly changing the results, which is not the case here. This can be understood in the following terms. Long-range magnetostatic interactions in crystalline ferromagnets are responsible for the formation of magnetic domains of size ranging from micrometers to millimeters depending on the geometry of the sample[15]. On the contrary, the RA leads to the formation of much smaller nanometer size Imry-Ma domains for which local interactions are dominant.

The effective exchange field acting on each spin from the nearest neighbors in d dimensions is $2dJs$. In our model it competes with the anisotropy field of strength $2sD_R$. The case of a large random anisotropy, $2sD_R \gg 2dJs$, that is, $D_R \gg dJ$, is obvious. It corresponds to a system of weakly interacting randomly oriented spins, each spin aligned with the local anisotropy axis $\mathbf{n}$. Due to the two equivalent directions along the easy axis the system possesses high metastability with the magnetic state depending on history.

On the contrary, weak anisotropy, $D_R \ll dJ$, cannot destroy the local ferromagnetic order created by the strong exchange interaction. The direction of the magnetization becomes only slightly disturbed when one goes from one lattice site to the other. As in the random walk problem, the deviation of the direction of the magnetization would grow with the distance. In a d-dimensional lattice of spacing a the average statistical fluctuation of the random anisotropy field per spin in a volume of size R scales as $D_{\text{eff}} = 2sD_R(a/R)^{d/2}$. Since Heisenberg exchange is equivalent to $J(\nabla\mathbf{s})^2$ in a continuous spin-field model, the ordering effect of the exchange field scales as $2dJs(a/R)^2$. The effective exchange and anisotropy energies become comparable at $R \sim R_f$, where

$$R_f \sim a(dJ/D_R)^{2/(4-d)} \quad (2)$$

determines the ferromagnetic correlation length. The exact numerical factor in front of $(dJ/D_R)^{2/(4-d)}$ is unknown but the existing approximations and numerical results suggest that it increases progressively with the dimensionality of the system[15,26].

Since magnetic anisotropy has relativistic origin its strength per spin is usually small compared to the exchange per spin. Anisotropy axes in the amorphous ferromagnet are determined by the local arrangement of atoms. When the latter has a short range order the axes are correlated within structurally ordered grains whose size must replace a in the RA model. This results in a greater effective RA, making both limits, $D_R \ll dJ$ and $D_R \gg dJ$, relevant to amorphous ferromagnets[14,16].

As to the Zeeman interaction of the ac field with the spins, that is determined by the amplitude of $\mathbf{h}$ in Eq. (1), in all situations of practical interest it would be smaller than all other interactions by many orders of magnitude. It is worth noticing, however, that for a sufficiently large system the random energy landscape created by the RA

and the ferromagnetic exchange would have all energy scales, including that of h. This, in principle, may inject nonlinearity into the problem with a however small amplitude of the ac field.

The dynamics of the system is given by the Landau-Lifshitz equation

$$\hbar\dot{\mathbf{s}}_i = \mathbf{s}_i \times \mathbf{h}_{\mathrm{eff},i} - \alpha \mathbf{s}_i \times (\mathbf{s}_i \times \mathbf{h}_{\mathrm{eff},i}), \quad \mathbf{h}_{\mathrm{eff},i} \equiv -\frac{\partial \mathcal{H}}{\partial \mathbf{s}_i} \quad (3)$$

that describes precession of the spin about the direction of the local effective field and relaxation towards it. Here, $\alpha \ll 1$ is the phenomenological damping constant. However, as will be discussed later, a random magnet has a continuous distribution of resonances (normal modes) that makes the power absorption insensitive to the small damping. Using the equation of motion above (see Appendix), one obtains the relation

$$\dot{\mathcal{H}}(t) = -\dot{\mathbf{h}}(t) \cdot \sum_i \mathbf{s}_i(t) - \frac{\alpha}{\hbar} \sum_i \left(\mathbf{s}_i(t) \times \mathbf{h}_{\mathrm{eff},i}\right)^2, \quad (4)$$

for the rate of change of the energy of the magnetic system. It equals the work of the ac field per unit time (absorbed power) minus the dissipated power. We define the change of the energy of the spin system and the absorbed energy of the ac field as time integrals

$$\Delta E = \int dt\, \dot{\mathcal{H}}(t), \quad E_{\mathrm{abs}} = -\int dt\, \dot{\mathbf{h}}(t) \cdot \sum_i \mathbf{s}_i(t), \quad (5)$$

respectively. For a conservative system ($\alpha = 0$) these two quantities coincide. They represent the two ways of calculating the absorbed power numerically, which is important for checking the self-consistency and accuracy of computations. In the presence of dissipation ($\alpha > 0$), these two quantities are different.

When the phenomenological damping is included, the energy of the spin system, and thus ΔE, saturate in a stationary state in which the power absorption is balanced by dissipation. On the contrary, the work done by the ac field, E_{abs}, continues to increase period after period of the ac field. In this case the rate of change of E_{abs} becomes the single measure of the absorbed power.

If the damping was due to the emission of electromagnetic waves by spins, then at large times the energy would saturate due to the detailed balance between absorption and emission of photons. However, in real systems the damping would be dominated by the interaction of spins with electrons and phonons, making re-emission of microwaves irrelevant. For a large system, a long computing time is needed to reach saturation, especially when the damping is small. Fortunately, in most cases the absorbed power can be already obtained with a good accuracy from a short computation on a conservative system, typically using 5 periods of the ac field.

One other complication arises from the necessity to keep the amplitude of the ac field as small as possible in relation to the exchange and anisotropy to reflect situations of practical interest. In this case, one can expect normal modes to respond to the ac field independently. However, decreasing the amplitude of the ac field below a certain threshold increases computational errors. Large amplitude of the ac field causes resonant group of the normal modes to oscillate at higher amplitudes, which triggers nonlinear processes of the energy conversion.

We use the following procedure. At the first stage, the magnetic state in zero field is prepared by the energy minimization starting from random orientation of spins. This reflects the process of manufacturing of amorphous ferromagnet by a rapid freezing from the paramagnetic state in the melt. The numerical method[34] combines sequential rotations of spins $\mathbf{s}_i$ towards the direction of the local effective field, $\mathbf{H}_{\mathrm{eff},i}$, with the probability η, and the energy-conserving spin flips (overrelaxation), $\mathbf{s}_i \to 2(\mathbf{s}_i \cdot \mathbf{H}_{\mathrm{eff},i})\mathbf{H}_{\mathrm{eff},i}/H^2_{\mathrm{eff},i} - \mathbf{s}_i$, with the probability $1-\eta$. We used $\eta = 0.03$ that ensures the fastest relaxation. At the end of this stage, a disordered magnetic state with the ferromagnetic correlation length R_f is obtained (see Fig. 1).

At the second stage, the ac field is turned on and Eq. (3) is solved with the help of the classical fourth-order Runge-Kutta method. We also have tried the 5th order Runge-Kutta method by Butcher[35] that makes six function evaluations per time step. This method can be faster as it allows a larger time step for the same accuracy. However, for the RA model it shows instability and has been discarded. The frequency dependence of the absorbed power was computed in a parallelized cycle over frequencies. For each frequency, the dynamical evolution was run up to five periods of the ac field. For the lowest frequencies, the computation was rather long. Wolfram Mathematica with compilation on a 20-core Dell Precision Workstation was used. In the computations, we set $s = \hbar = J = 1$, which corresponds to energy in the units of J and time in the units of $\hbar/J$. In most cases the integration step was $\Delta t = 0.1$ or 0.05. We computed the absorbed power in 1D, 2D, and 3D systems with a number of spins N up to $400,000$ in 3D.

In three dimensions, the ferromagnetic correlation length at small D_R is very large and can easily become longer than the system size. In this case, the magnetization per spin $m = |\mathbf{m}|$, where $\mathbf{m} \equiv (1/N)\sum_i \mathbf{s}_i$ is the average spin polarization, may be far from zero at the energy minimum. For the sake of uniformity, the ac field was always applied in the direction perpendicular to $\mathbf{m}$ for which the power absorption is stronger than in the direction parallel to $\mathbf{m}$. The absorbed power P_{abs} was obtained by numerically integrating the left or right side of Eq. (4) during N_T periods of the ac field and dividing the result by $N_T T$ with $T = 1/f = 2\pi/\omega$. In most cases we used $N_T = 5$. All time-dependent results are represented for the times equal to the multiples of the half-period of the ac pumping for which $\sin(\omega t) = 0$ and thus the Zeeman term due to the ac field does not add up to the energy of the magnetic system. It was numerically confirmed that $P_{\mathrm{abs}} \propto h_0^2$, so, in the plots we show P_{abs}/h_0^2 per spin.

III. NUMERICAL RESULTS

To test our short-time method of computing the absorbed power, we performed longer computations and plotted the absorbed energy vs time for the integer number of periods of the ac field, $t = nT$, $n = 0, 1, 2, \ldots$ For the undamped model, $\alpha = 0$, both methods of computing the absorbed energy discussed in the previous section give the same result, which proves sufficient computational accuracy. For the damped model, the energy of the system saturates at long times while the magnetic work, obtained by integrating the right-hand side of Eq. (4) continues to increase linearly.

An example of these tests is shown in Fig. 2 for a 2D system of 300×300 spins with $D_R/J = 1$, $\hbar\omega/J = 0.2$, the ac-field amplitude $h_0/J = 0.01$, and different values of the damping constant α. For the unrealistically high damping $\alpha = 0.1$ the absorbed energy line goes higher than the other dependencies. For $\alpha = 10^{-2}$, 10^{-3}, and 10^{-4} the magnetic work is practically the same. This confirms our conjecture about a continuous distribution of resonances for which the absorption does not depend of the resonance linewidths, see the next section. In the undamped case, $\alpha = 0$, the absorbed energy goes lower at large times which indicates saturation of resonances at a given amplitude of the ac-field.

An important finding of these numerical experiments is that the absorbed energy increases nearly linearly in time, that is, the absorbed power is practically time independent. This allows one to use a small number of periods, $N_T = 5$ or 10, in the computation of the absorbed power at different frequencies for different system dimensionalities. Still, computations for large systems and low frequencies are rather long.

Short time intervals lead to the broadening: $\Delta\omega \sim 1/t = 1/(N_T T) = \omega/(2\pi N_T)$. For $N_T = 5$ one obtains $\Delta\omega \sim 0.03\omega$, a rather small broadening given that the absorption spectrum is broad and the computations are performed over many decades of the frequency ω of the ac field. Computations with $N_T = 10$ produced essentially the same results as computations with $N_T = 5$. As an illustration, one can consider a pumped harmonic oscillator with the energy $(m/2)\left(\dot{x}^2 + \omega_0^2 x^2\right) - x f_0 \sin(\omega t)$, described by the equation of motion $\ddot{x} + 2\Gamma\dot{x} + \omega_0^2 x = (f_0/m)\sin(\omega t)$ with low damping, $\Gamma \ll \omega_0$. At short times, $\Gamma t \ll 1$, the absorbed power (rate of energy change) is given by

$$P_{\rm abs} = \frac{f_0^2 t}{2m} \frac{1 - \cos\left[(\omega - \omega_0)\, t\right]}{\left[(\omega - \omega_0)\, t\right]^2}. \qquad (6)$$

The width of the peak in the absorption decreases with the measurement time as $\Delta\omega \sim 1/t$, while its height grows linearly with t, so that its integral intensity is independent of time. For a broad distribution of the oscillators' frequencies ω_0, this function can be replaced by $P_{\rm abs} \approx \left[f_0^2/(2m)\right] \pi\delta(\omega - \omega_0)$. This is the limit in which computations reported here have been performed.

Given the weak dependence of the absorption on the damping at small α the bulk of our results were obtained for $\alpha = 0$. The choice of the amplitude of the ac-field is important for numerical work. Large h_0 reduces numerical noise while leading to the flattening of the absorption maxima due to a partial saturation. Small h_0 increases computational errors. We have chosen the values $h_0/J = 0.0001$ in 1D (where numerical errors are the smallest), $h_0/J = 0.0003$ in 2D, and $h_0/J = 0.003$ in 3D.

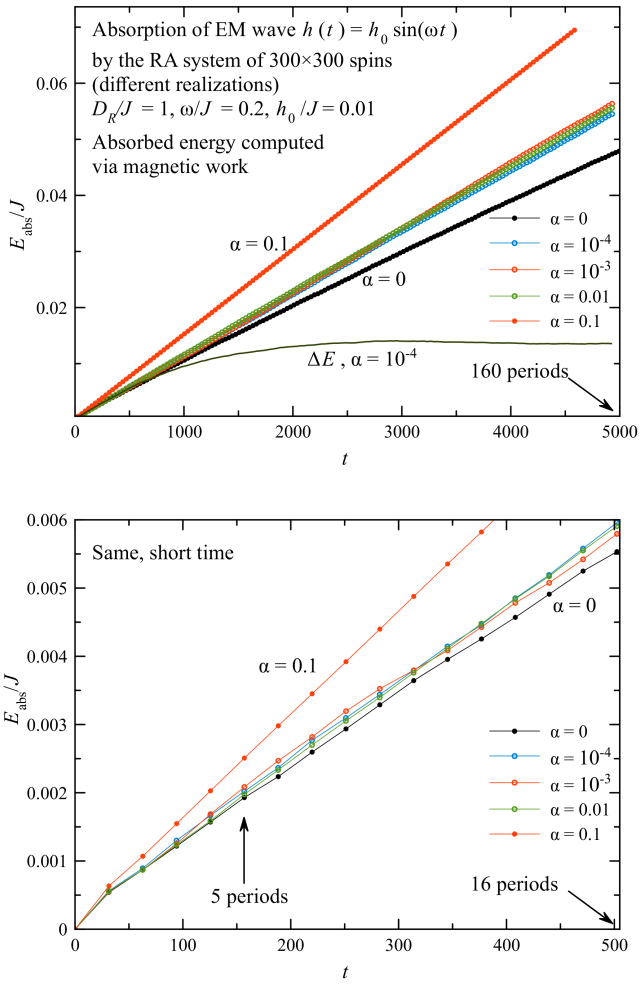

Figure 2: Upper panel: Absorbed energy of the ac field vs time for a 2D system of 300×300 spins for different values of the damping constant. The energy increase ΔE of the magnetic system caused by the ac power absorption, that saturates at long times due to dissipation, is shown at $\alpha = 10^{-4}$. The short-time dependence of the absorbed power is the same in all cases except for that of the largest damping. Lower panel: The short-time dependence of the absorbed energy shows that the slope that determines the power absorption is nearly constant and can be established with good accuracy after 5 periods of the ac field.

The frequency dependence of the absorbed power for in a 1D RA ferromagnet is shown in Fig. 3. This is the

easiest case computationally. One can use a long chain of spins (here $N = 30000$) that is much longer than the magnetic correlation radius R_f in 1D. Thus, after the energy minimization the system remains well disordered, $m \ll 1$. Fig. 3 shows broad absorption maxima shifting to lower frequencies with decreasing D_R. The heights of the maxima are approximately the same. At large frequencies, there is a cut-off at the highest spin-wave frequency, $\omega_{\max} = 4dJ \Rightarrow 4J$ in 1D.

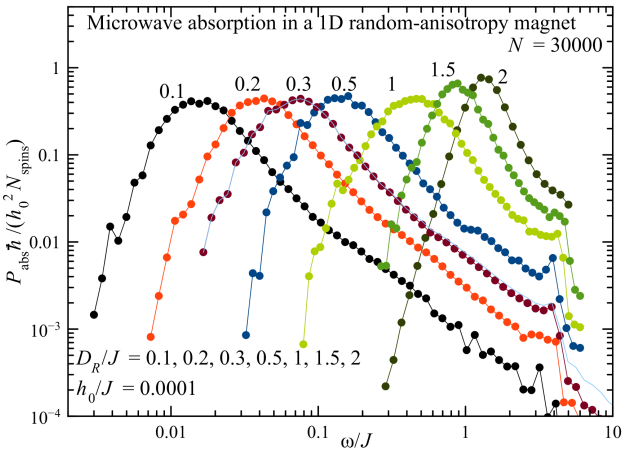

Figure 3: Absorbed power vs ω for different values of the random anisotropy D_R in 1D.

Frequency dependence of the absorbed power for the 2D model is shown in Fig. 4. Qualitatively the results are the same as in 1D, only we used a larger system of $N = 340 \times 300 = 102000$ spins. Here, we were able to go down to the RA only as small as $D_R/J = 0.2$ as compared to 0.1 in 1D because the absorption maximum is shifting to very low frequencies on decreasing RA.

Frequency dependence of the absorbed power for the 3D model is shown in Fig. 5. In the range of D_R/J that is reliably accessible numerically, the absorption curves are similar to 1D and 2D. However, the 3D model is the hardest to crack numerically because the ferromagnetic correlation length R_f, given by Eq. (2) with $d = 3$, becomes very large at small D_R. We had to use 3D systems of a much greater number of spins, $68 \times 74 \times 80 = 402560$, but of smaller lateral dimensions than 1D and 2D systems that we have studied. The lowest RA for which we could observe the absorption maximum in 3D was $D_R/J = 2$. For lower D_R the absorption maxima shift to very low frequencies for which computation becomes impractically long and inhibited by the accumulation of numerical errors.

Frequency dependence of the power on the right side of the absorption maximum allows scaling shown in Fig. 6. We have found that $P(\omega)$ in this region follows the

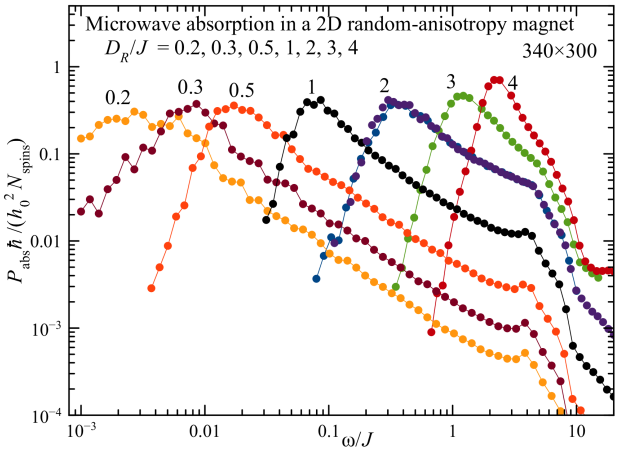

Figure 4: Absorbed power vs ω for different values of the random anisotropy D_R in 2D.

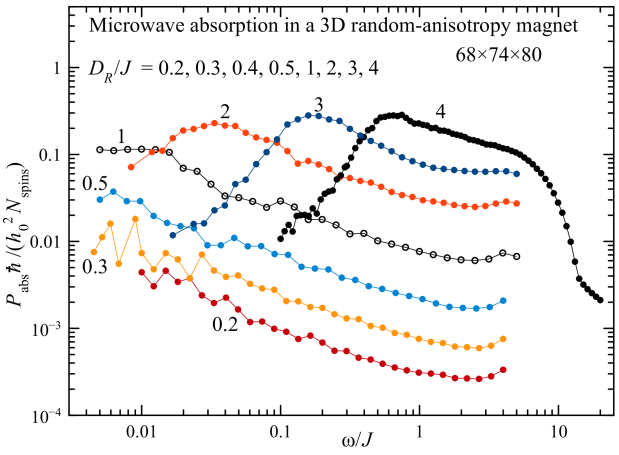

Figure 5: Absorbed power vs ω for different values of the random anisotropy D_R in 3D.

power law:

$$P_{\rm abs} \propto \frac{D_R^2}{J^2} \left(\frac{J}{\hbar\omega} \right)^{(4-d)/2} . \qquad (7)$$

up to the high-frequency cutoff determined by the strength of the exchange interaction. Away from the maximum the absorption in this high-frequency region is lower in higher dimensions. However the heights of the absorption maxima are comparable in all dimensions, see figures 3, 4, and 5. The maximum absorption has weak dependence on the strength of the RA and the strength of the exchange interaction. By order of magnitude it is given by $P_{\max} \sim h_0^2 N/\hbar$.

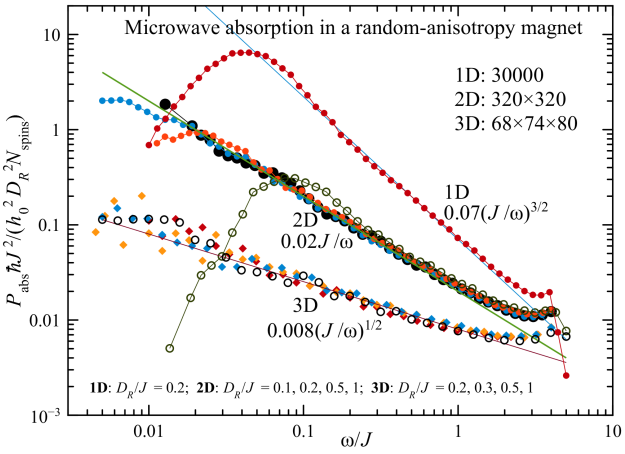

Figure 6: Scaling representation of the absorbed power at high frequencies for $d = 1, 2, 3$.

IV. INTERPRETATION OF THE RESULTS

A. Independence of the phenomenological damping

One noticeable feature of the ac power absorption by the RA magnet is its independence of the damping within a broad range of the damping constant $\alpha \ll 1$, see Fig. 2. It can be understood along the lines of the qualitative argument presented below.

The absorption power by a conventional ferromagnet near the FMR frequency, $\omega \approx \omega_0$, has a general form[15]

$$P(\omega, \omega_0, \alpha) \propto h_0^2 \omega_0^2 \frac{\alpha \omega_0^2 G}{(\omega^2 - \omega_0^2)^2 + (\alpha \omega_0^2 G)^2} \qquad (8)$$

with G being a geometrical factor depending on the polarization of the ac-field and the structure of the magnetic anisotropy. In the amorphous magnet, parameters ω_0 and G are broadly distributed due to the distribution of the magnitude and the direction of the effective RA. At $\alpha \to 0$ Eq. (8) becomes

$$P(\omega, \omega_0) \propto h_0^2 \omega_0^2 \delta(\omega^2 - \omega_0^2) \propto h^2 \omega_0 \delta(\omega - \omega_0). \qquad (9)$$

Assuming the distribution function $f(\omega_0)$ for the resonances, satisfying

$$\int d\omega_0 f(\omega_0) = 1, \qquad (10)$$

one obtains for the power absorption at a frequency ω

$$P(\omega) \propto \int d\omega_0 f(\omega_0) h_0^2 \omega_0 \delta(\omega - \omega_0) = h_0^2 \omega f(\omega) \qquad (11)$$

which is independent of α.

In fact, Eq. (8) is valid at the times longer than the relaxation time so that the stationary state of the system is achieved. In this work, to the contrary, short times are used, for which the relaxation can be neglected and absorption in the magnetic system is described by a formula similar to Eq. (6) for the undamped harmonic oscillator. Nevertheless, for a broad distribution of ω_0, both formulas can be replaced by the same frequency delta-function $\propto \delta(\omega - \omega_0)$, so that one obtains the same result.

The function $f(\omega_0)$ for the RA magnet is unknown. It is related to a more general poorly understood problem of excitation spectrum of systems characterized by a random potential landscape that we are not attempting to solve here. Based upon our numerical results, an argument can be made, however, that sheds light on the physics of the absorption by the RA magnet, see below.

B. Estimation of the maximum-absorption frequency

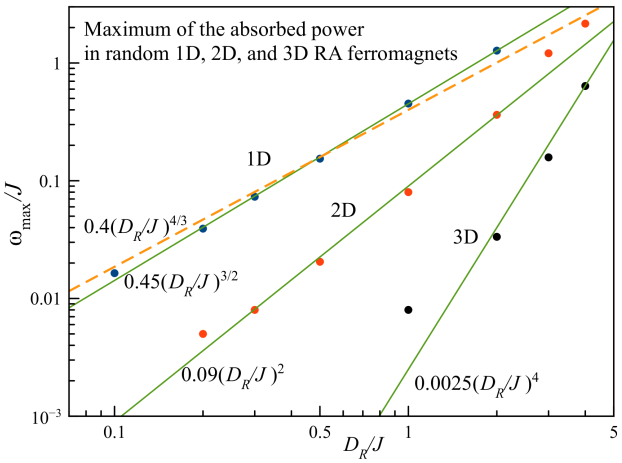

Figure 7: Peak absorption frequency vs strength of the RA. Points: numerical experiment. Lines: Power-law fits. In 1D, the expected power law 4/3 is shown by the dashed line while the best fit 3/2 is shown by a solid line.

The spin field in the RA ferromagnet, see Fig. (1), resembles to a some degree a domain structure or magnetization of a sintered magnet comprised of densely packed single-domain magnetic particles. The essential difference is the absence of boundaries between IM domains. They are more of a reflection of the disordering on the scale R_f than the actual domains. If one nevertheless thinks of the IM domains as independent ferromagnetically ordered regions of size R_f, their FMR frequencies, in the absence of the external field, would be dominated by the effective magnetic anisotropy, $D_{\rm eff}$, due to statistical fluctuations in the distribution of the RA axes. In this case the most probable resonance frequency that determines the maximum of $P(\omega)$ must be given by

$$\omega_{\max} \sim D_{\rm eff} \sim D_R (a/R_f)^{d/2}. \qquad (12)$$

Substituting here $R_f/a \sim k(d)(J/D_R)^{2/(4-d)}$, with the factor $k(d)$ increasing[14] progressively with d, we obtain

$$\frac{\omega_{\max}}{J} = \frac{1}{k^{d/2}} \left(\frac{D_R}{J}\right)^{4/(4-d)} . \qquad (13)$$

It suggests that $\omega_{\max}/J$ must scale as $(D_R/J)^{4/3}$ in one dimension, as $(D_R/J)^2$ in two dimensions, and as $(D_R/J)^4$ in three dimensions. For typical parameters of RA magnets[17] $\omega_{\max}$ falls in the microwave range.

The dependence of $\omega_{\max}/J$ on D_R/J for $d = 1, 2, 3$ derived from figures 3, 4, and 5 is shown in Fig. 7. In 2D and 3D there is a full agreement with the above argument. In 1D the best fit seems to be the 3/2 power of D_R/J instead of the expected 4/3 power. Given the qualitative nature of the argument presented above and good fit for $d = 2, 3$ the agreement is nevertheless quite good. The small factor in front of the power of D_R/J, that becomes progressively smaller as one goes from $d = 1$ to $d = 3$, correlates with the established fact[14,36] that $k(d)$ increases with d.

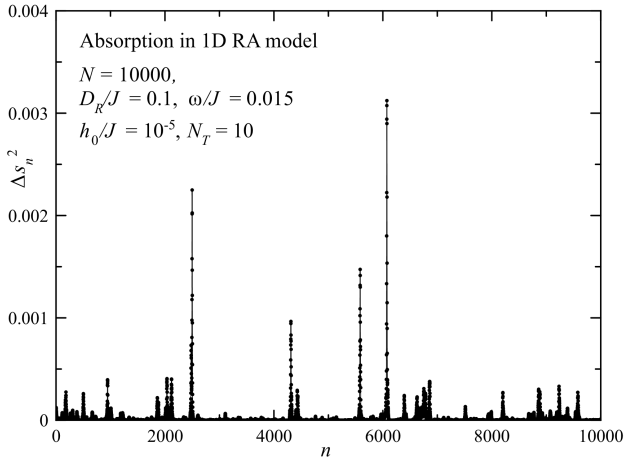

Figure 8: Spatial dependence of spin deviations in a 1D RA ferromagnet after $N_T = 10$ periods of ac pumping.

C. Visualization of the local dynamical modes

Further evidence of the validity of our picture that the power absorption occurs inside resonant IM domains comes from the analysis of the spatial dependence of local spin deviations from the initial state $s_i^{(0)}$, defined as $\Delta s_i^2 = (s_i - s_i^{(0)})^2$. They are related to local spin oscillations induced by the ac field and are illustrated in Fig. 8 for a 1D RA ferromagnet with $D_R/J = 0.1$ at the frequency $\omega/J = 0.015$ that corresponds to the absorption maximum (see Fig. 3). Noticeable spin deviations occur at multiple discrete locations. Their amplitude is apparently determined by how well the frequency of the ac field matches the resonant frequency of the IM domain at that location. The oscillating domains appear to be well separated in space. Their positions depend on frequency in a random manner because for each frequency there is a different resonant domain and there is no clear correlation between positions of domains corresponding to close frequencies.

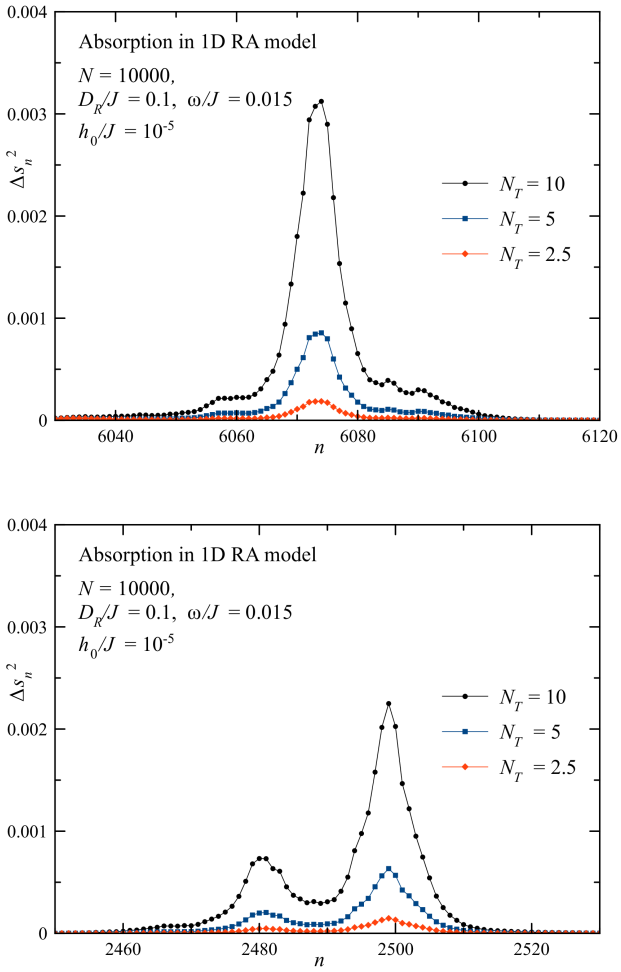

Figure 9: Spatial dependence of spin deviations in one areas of resonant absorption at different moments of time: $N_T = 2.5, 5, 10$ periods of ac pumping. Upper panel: The highest peak at $n = 6074$ in Fig. 8 zoomed in; Lower panel: The second-highest peak at $n = 2499$ zoomed in.

Two regions of maximal spin deviations of Fig. 8 are zoomed at in Fig. 9. It shows that the amplitude of resonant spin oscillations steadily grows with time. Spin deviations rapidly disappear away from the maximum. For the frequency $\omega/D_R = 0.015$, the widths of these regions is of order $10a$ which roughly agrees with the 1D ferromagnetic correlation length computed in Ref. 36. Up to the unknown factor of order unity it is also in agreement with the expected relation (12) between R_f and the resonant frequency. Time dependence of the spin

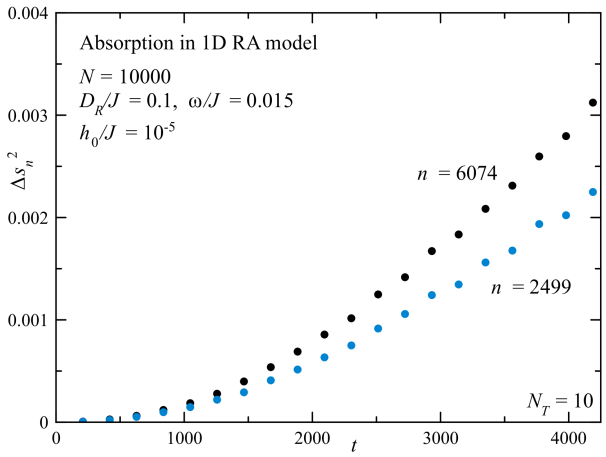

Figure 10: Time dependence of the heights of the largest and second-largest absorprion peaks in the preceding figures.

deviations at these two spatial maxima is plotted in Fig. 10.

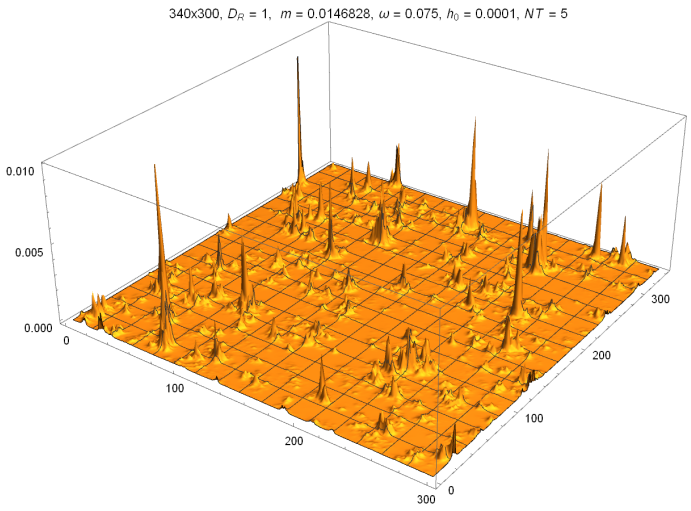

Figure 11: Spatial dependence of spin deviations in a 2D RA ferromagnet after $N_T = 5$ periods of ac pumping.

Fig. 11 shows oscillating regions in a 2D RA ferromagnet. Here again the spin regions that absorb the ac power are well separated in space. This is in line with our picture of resonant IM domains in which the effective magnetic anisotropy due to statistical fluctuations of easy axis directions matches the frequency of the ac field. The peaks in figures 8, 9, and 11 grow in time, as the energy is absorbed.

At present we do not have the full theory of the frequency dependence of the absorbed power. Apparently, it is related to the size distribution of ferromagnetically correlated regions (Imry-Ma domains), which remains a challenging unsolved problem of statistical mechanics. Our numerical findings, however, may shed some partial light on this problem.

Indeed, we have found that at large frequencies the power absorption follows Eq. (7): $P \propto \omega^{(d/2)-2}$. If it is related to the precession of IM domains of size R, then according to Eq. (12) the frequency of this precession scales as $\omega \propto R^{-d/2}$. Since this is a high-frequency regime, it must correspond to small R. According to Eq. (11) $P \propto \omega f(\omega)$. Combined with Eq. (7) it gives $f(\omega) \propto \omega^{(d/2)-3}$ at large ω. If distribution of IM domains is given by $F(R)$ satisfying $\int dRF(R) = \int d\omega f(\omega) = 1$, then, using the above formulas we obtain

$$F(R) = f(\omega)\frac{d\omega}{dR} \propto R^{-\left(\frac{d}{2}-1\right)^2}. \qquad (14)$$

This suggests $R^{-1/4}$ distribution of small-size IM domains in 1D and 3D, and independence of R (up to a log factor) in 2D.

The qualitative argument leading to Eq. (14) is based upon the picture of independently oscillating IM domains. In reality there are no boundaries between ferromagnetically correlated regions. Our derivation suggests a large fraction of compact correlated regions of size that is small compared to the ferromagnetic correlation length R_f. It is supported by Fig. 1 but is different from the prediction of the exponentially small number of such regions in the random-field xy model made within the variational approach[37].

V. DISCUSSION

We have studied the power absorption by the random-anisotropy ferromagnet in a microwave field in one, two, and three dimensions. The one-dimensional problem describes a thin wire of diameter smaller than the 1D ferromagnetic correlation length R_f and of length greater than R_f. The two-dimensional problem corresponds to a film of thickness that is small compared to the 2D ferromagnetic correlation length and of lateral dimension large compared to R_f. The three-dimensional problem corresponds to a particle of amorphous ferromagnet of size large compared to the 3D ferromagnetic correlation length.

Our main finding agrees with the statements made by experimentalists[9]. It elucidates the physics of the microwave absorption by an RA ferromagnet. The absorption is localized inside well separated regions. Scaling of the peak absorption frequency with the strength of the RA points towards the mechanism of the absorption in which oscillations of spins are dominated by isolated ferromagnetically correlated regions (Imry-Ma domains) that are in resonance with the microwave field.

Broad distribution of sizes of ferromagnetically correlated regions results in the broad distribution of resonance frequencies. It makes the absorption broadband. In 1D and 2D systems the linewidth at half-height is close

to the frequency $\omega_{\max}$ that provides the absorption maximum. The linewidth is greater than $\omega_{\max}$ in a 3D system. Another consequence of the broad distribution of resonance frequencies is independence of the absorption on the damping of spin oscillations within a few orders of magnitude of the damping constant.

A remarkable observation is that the maximum of the absorbed power in a random magnet has a weak dependence on basically all parameters of the system, such as dimensionality, damping, the strength of the RA, and the strength of the exchange interaction. By the order of magnitude it is determined solely by the total number of spins absorbing the microwave energy and the amplitude of the microwave field. This again is a consequence of the broad distribution of sizes of ferromagnetically correlated regions, causing broad distribution of the effective magnetic anisotropy and effective exchange interaction.

A practical question is whether the RA (amorphous) magnets have a good prospect as microwave absorbers. Frequencies that provide the maximum of the absorption depend on the strength of the RA. The latter can be varied by at least two orders of magnitude by choosing soft or hard magnetic materials in the process of manufacturing an amorphous magnet. It must allow the peak absorption in the range from a few GHz to tens of GHz.

Rigorous computation of the fraction of the incoming microwave power absorbed by the system depends on its composition and boundary conditions but an order of magnitude estimate can be made based upon the following simple argument. One of our findings is that the power absorption at frequencies near the absorption maximum depends weakly on the parameters of the RA ferromagnet, see Figs. 3 - 5. By order of magnitude it equals $P_{\max} \sim 4(1+\chi)\mu_B^2 s^2 B_0^2 n_0 A d/\hbar$ in terms of the length of the dimensionless spin s and the dimensional amplitude, B_0, of the microwave field, with χ being the magnetic susceptibility and μ_B being the Bohr magneton. Here we introduced concentration of spins n_0, the area A and the thickness d of the absorbing layer. Since the incoming microwave delivers to the layer the power $P_m = (cB_0^2/2\mu_0)A$, with μ_0 being the permeability of free space[38], we obtain $P_{\max}/P_m \sim 8s^2(1+\chi)\mu_0\mu_B^2 n_0 d/(\hbar c)$. This ratio is assumed to be smaller than one. When it reaches unity on increasing d this means that the microwave power would be totally absorbed by a thicker layer. Given large susceptibilities exhibited by the RA magnets[17], this regime may, in principle, be achieved in a dielectric layer of a few millimeter thickness densely packed with coated microscopic amorphous wires, foils, and particles.

Acknowledgements

This work has been supported by the grant No. 20RT0090 funded by the Air Force Office of Scientific Research.

Appendix: Absorption of the ac field by a magnetic system

The energy of the classical-spin system under the action of the ac field can be written as

$$\mathcal{H}(t) = -\mathbf{h}(t)\cdot\sum_i \mathbf{s}_i(t) + \mathcal{H}_0(t), \tag{15}$$

where $\mathbf{h}(t)$ is the ac field and $\mathcal{H}_0(t)$ is the rest of the energy of the magnetic system. Due to the action of the ac field (as well as other factors), orientation of spins depends on time. The time derivative of the energy is

$$\begin{aligned}\dot{\mathcal{H}}(t) &= -\dot{\mathbf{h}}(t)\cdot\sum_i \mathbf{s}_i(t) - \mathbf{h}(t)\cdot\sum_i \dot{\mathbf{s}}_i(t) + \dot{\mathcal{H}}_0(t)\\ &= -\dot{\mathbf{h}}(t)\cdot\sum_i \mathbf{s}_i(t) - \mathbf{h}(t)\cdot\sum_i \dot{\mathbf{s}}_i(t) - \sum_i \mathbf{H}_{\mathrm{eff},i}\cdot\dot{\mathbf{s}}_i(t)\\ &= -\dot{\mathbf{h}}(t)\cdot\sum_i \mathbf{s}_i(t) - \sum_i \mathbf{h}_{\mathrm{eff},i}(t)\cdot\dot{\mathbf{s}}_i(t),\end{aligned} \tag{16}$$

where

$$\mathbf{H}_{\mathrm{eff},i} \equiv -\frac{\partial\mathcal{H}_0}{\partial\mathbf{s}_i}, \qquad \mathbf{h}_{\mathrm{eff},i} \equiv \mathbf{h} + \mathbf{H}_{\mathrm{eff},i} = -\frac{\partial\mathcal{H}}{\partial\mathbf{s}_i}. \tag{17}$$

The time derivative of the spin vector is given by the equation of motion (3) or, equivalently, by

$$\hbar\dot{\mathbf{s}}_i(t) = \mathbf{s}_i(t)\times\mathbf{h}_{\mathrm{eff},i} - \alpha\left[\mathbf{s}_i(t)\left(\mathbf{s}_i(t)\cdot\mathbf{h}_{\mathrm{eff},i}\right) - \mathbf{h}_{\mathrm{eff},i}s^2\right]. \tag{18}$$

This gives

$$\dot{\mathcal{H}}(t) = -\dot{\mathbf{h}}(t)\cdot\sum_i \mathbf{s}_i(t) - \frac{\alpha}{\hbar}\sum_i\left[s^2h_{\mathrm{eff},i}^2 - \left(\mathbf{s}_i(t)\cdot\mathbf{h}_{\mathrm{eff},i}\right)^2\right], \tag{19}$$

or, finally,

$$\dot{\mathcal{H}}(t) = -\dot{\mathbf{h}}(t)\cdot\sum_i \mathbf{s}_i(t) - \frac{\alpha}{\hbar}\sum_i\left(\mathbf{s}_i(t)\times\mathbf{h}_{\mathrm{eff},i}\right)^2. \tag{20}$$

[1] P. Monod and Y. Berthier, Zero field electron spin resonance of Mn in the spin glass state, Journal of Magnetism and Magnetic Materials **15-18**,149-150 (1980); J. J. Prejean, M. Joliclerc, and P. Monod, Hysteresis in CuMn : The effect of spin orbit scattering on the anisotropy in the spin glass state, Journal de Physique (Paris) **41**, 427-435 (1980). I

[2] H. Alloul and F. Hippert, Macroscopic magnetic anisotropy in spin glasses: transverse susceptibility and zero field NMR enhancement, Journal de Physique Lettres

41, L201-204 (1980).

[3] S. Schultz, E .M. Gulliksen, D. R. Fredkin, and M.Tovar, Simultaneous ESR and magnetization measurements characterizing the spin-glass State, Physical Review Letters **45**, 1508-1512 (1980); E. M. Gullikson, D. R. Fredkin, and S. Schultz, Experimental demonstration of the existence and subsequent breakdown of triad dynamics in the spin-glass CuMn, Physical Review Letters **50**, 537-540 (1983). I

[4] A. Fert and P. M. Levy, Role of anisotropic exchange interactions in determining the properties of spin-glasses, Physical Review Letters **44**,1538-1541 (1980); P. M. Levy and A. Fert, Anisotropy induced by nonmagnetic impurities in CuMn spin-glass alloys, Physical Review B **23**, 4667 (1981). I

[5] C. L. Henley, H. Sompolinsky, and B. I. Halperin, Spin-resonance frequencies in spin-glasses with random anisotropies, Physical Review B **25**, 5849-5855, (1982). I

[6] B. I. Halperin and W. M. Saslow, Hydrodynamic theory of spin waves in spin glasses and other systems with noncollinear spin orientations, Physical Review B **16**, 2154-2162 (1977). I

[7] W. M. Saslow, Anisotropy-triad dynamics, Physical Review Letters **48**, 505-508 (1982). I

[8] G. Suran, E. Boumaiz, and J. Ben Youssef, Experimental observation of the longitudinal resonance mode in ferromagnets with random anisotropy, Journal of Applied Physics 79, 5381 (1996); S. Suran and E. Boumaiz, Observation and characteristics of the longitudinal resonance mode in ferromagnets with random anisotropy, Europhysics Letters **35**, 615-620 (1996). I

[9] S. Suran and E. Boumaiz, Longitudinal resonance in ferromagnets with random anisotropy: A formal experimental demonstration, Journal of Applied Physics **81**, 4060 (1997); G. Suran, Z, Frait, and E. Boumaz, Direct observation of the longitudinal resonance mode in ferromagnets with random anisotropy, Physical Review B **55**, 11076-11079 (1997); S. Suran and E. Boumaiz, Longitudinal-transverse resonance and localization related to the random anisotropy in a-CoTbZr films, Journal of Applied Physics **83**, 6679 (1998) I, V

[10] W. M. Saslow and C. Sun, Longitudinal resonance for thin film ferromagnets with random anisotropy, Physical Review B **98**, 214415-(6) (2018). I

[11] R. D. McMichael, D. J. Twisselmann, and A. Kunz, Localized ferromagnetic resonance in inhomogeneous thin film, Physical Review Letters **90**, 227601-(4) (2003). I

[12] G. de Loubens, V. V. Naletov, O. Klein, J. Ben Youssef, F. Boust, and N. Vukadinovic, Magnetic resonance studies of the fundamental spin-wave modes in individual submicron Cu/NiFe/Cu perpendicularly magnetized disks, Physical Review Letters **98**, 127601-(4) (2007). I

[13] C. Du, R. Adur, H. Wang, S. A. Manuilov, F. Yang, D. V. Pelekhov, and P. C. Hammel, Experimental and numerical understanding of localized spin wave mode behavior in broadly tunable spatially complex magnetic configurations, Physical Review B **90**, 214428-(10) (2014). I

[14] E. M. Chudnovsky, W. M. Saslow, and R. A. Serota, Ordering in ferromagnets with random anisotropy, Physical Review B **33**, 251-261 (1986). I, II, II, IV B, IV B

[15] E. M. Chudnovsky and J. Tejada, *Lectures on Magnetism* (Rinton Press, Princeton, New Jersey, 2006). II, II, IV A

[16] T. C. Proctor, E. M. Chudnovsky, and D. A. Garanin, Scaling of coercivity in a 3d random anisotropy model, Journal of Magnetism and Magnetic Materials, **384**, 181-185 (2015). I, I, II

[17] E. M. Chudnovsky, Random Anisotropy in Amorphous Alloys, Chapter 3 in the Book: *Magnetism of Amorphous Metals and Alloys*, edited by J. A. Fernandez-Baca and W.-Y. Ching, pages 143-174 (World Scientific, Singapore, 1995). I, II, IV B, V

[18] A. I. Larkin, Effect of inhomogeneities on the structure of the mixed state of superconductors, Soviet Physics JETP **31**, 784-786 (1970). I

[19] Y. Imry and S.-k. Ma, Random-field instability of the ordered state of continuous symmetry, Physical Review Letters **35**, 1399-1401 (1975). I

[20] S. Fishman and A. Aharony, Random field effects in disordered anisotropic antiferromagnets, Journal of Physics C: Solid State Physics **12**, L729-L733 (1979). I

[21] G. Blatter, M. V. Feigel'man, V. B. Geshkenbein, A. I. Larkin, and V. M. Vinokur, Vortices in high temperature superconductors, Review of Modern Physics **66**, 1125-1388 (1994). I

[22] G. Grüner, The dynamics of charge-density waves, Review of Modern Physics **60**, 1129-1181 (1988). I

[23] T. Bellini, N. A. Clark, V. Degiorgio, F. Mantegazza, and G. Natale, Physical Review E **57**, 2996-3006 (1998). I

[24] Q. Zhang and L. Radzihovsky, Smectic order, pinning, and phase transition in a smectic-liquid-crystal cell with a random substrate, Physical Review E **87**, 022509-(25) (2013). I

[25] G. E. Volovik, On Larkin-Imry-Ma state in ^{3}He-A in aerogel, Journal of Low Temperature Physics **150**, 453-463 (2008). I

[26] T. C. Proctor, D. A. Garanin, and E. M. Chudnovsky, Random fields, Topology, and Imry-Ma argument, Physical Review Letters **112**, 097201-(4) (2014). I, II, II

[27] E. M. Chudnovsky and D. A. Garanin, Topological order generated by a random field in a 2D exchange model, Physical Review Letters **121**, 017201-(4) (2018). I

[28] D. A. Garanin and E. M. Chudnovsky, Ordered vs. disordered states of the random-field model in three dimensions, European Journal of Physics B **88**, 81-(19) (2015). I

[29] I. Y. Korenblit and E. F. Shender, Spin glasses and nonergodicity, Soviet Physics Uspekhi bf 32, 139-162 (1989). I

[30] J. V. I. Jaakko et al., Magnetic nanocomposites at microwave frequencies, in a book: *Trends in Nanophysics*, edited by V. Barsan and A. Aldea, pages 257-285 (Springer, New York, 2010). I

[31] G. Sun, B. Dong, M. Cao, B. Wei, and C. Hu, Hierarchical dendrite-like magnetic materials of Fe_3O_4, γ-Fe_2O_3, and Fe with high performance of microwave absorption, Chemistry of Materials **23**, 1587-1593 (2011). I

[32] F. Mederos-Henry et al., Highly efficient wideband microwave absorbers based on zero-valent Fe@γ-Fe_2O_3 and Fe/Co/Ni carbon-protected alloy nanoparticles supported on reduced graphene oxide, Nanomaterials **9**, 1196-(19) (2019).

[33] X. Zeng, X. Cheng, R. Yu, and G. D. Stucky, Electromagnetic microwave absorption theory and recent achievements in microwave absorbers, Carbon **168**, 606-623 (2020). I

[34] D. A. Garanin, T. C. Proctor, and E. M. Chudnovsky, Random field xy model in three dimensions, Physical Review B **88**, 224418-(21) (2013). II

[35] J. C. Butcher, On fifth order Runger-Kutta methods, BIT Numerical Mathematics **35**, 202-209 (1995). II

[36] R. Dickman and E. M. Chudnovsky, XY chain with random anisotropy: Magnetization law, susceptibility, and correlation functions at $T = 0$, Physical Review B **44**, 4397-4405 (1991). IV B, IV C

[37] T. Garel, G. Lori, and H. Orland, Variational study of the random-field XY model, Physical Review B **53**, R2941-R2944 (1996). IV C

[38] J. D. Jackson, *Classical Electrodynamics*, Third Edition (Willey & Sons, New York, 1998).

V